Nonradiative recombination via deep impurity levels in semiconductors: The excitonic Auger mechanism

Andreas Hangleiter
Physikalisches Institut, Universität Stuttgart,
Pfaffenwaldring 57, D-7000 Stuttgart 80, Federal Republic of Germany
(Received 2 September 1986; revised manuscript received 24 August 1987)

We present a theoretical investigation of excitonic Auger recombination via deep impurity levels in semiconductors. A calculation of the transition matrix elements is carried out for several levels of approximation. The influence of carrier density and temperature is studied by taking into account the screening of the Coulomb interaction at high carrier densities and the thermal ionization of the excitons. The results of our calculations are then compared to our experimental results, which originally led to the development of our model of excitonic Auger recombination via deep impurities.

I. INTRODUCTION

It is generally accepted[1] that the recombination of excess charge carriers via deep impurity levels in semiconductors occurs by a two-step process where electrons and holes are captured successively into the deep level. The model of Shockley and Read[2] and Hall[3] (SRH) accounts for this two-step nature of the recombination and yields a good description of the basic recombination kinetics. Within this model, however, the physical mechanism of the capture process remains unsolved. There have been numerous attempts, experimentally as well as theoretically, to solve this open question.[4–13]

In a preceding paper[14] we have presented our experimental results on nonradiative recombination via deep impurity levels in silicon. We have shown that none of the previously proposed models for capture into deep levels, namely multiphonon capture,[5] cascade capture,[15,6] or Auger capture of free carriers,[7–11] can account for the experimental facts. From our experimental data, especially from a direct proof of Auger recombination via the deep level,[14,16] we have developed a new model for deep level recombination, the model of excitonic Auger recombination via deep impurities.[14] The model is based on the fact that a free exciton meeting the impurity site always contains one particle to be captured, e.g., an electron, and one particle to take over the excess energy in an Auger process (e.g., a hole). Due to the spatial correlation of the electron and the hole within the exciton a very efficient excitonic Auger capture mechanism becomes possible. Since free excitons exist in thermal equilibrium with free electrons and holes, excitonic Auger recombination can give a significant contribution to the nonradiative recombination via deep levels.

Previously, only Auger capture processes of free electrons and holes at deep impurities and the Auger decay of excitons bound to the impurities have been considered. Landsberg *et al.*,[7] Robbins and Landsberg,[8] Haug,[9,10] Robbins,[11] Neumark,[12] and Riddoch and Jaros[13] have studied free-carrier Auger processes involving deep traps, whereas Auger recombination of excitons bound to shallow impurities were investigated by Nelson *et al.*,[17] Schmid,[18] and Lyon *et al.*[19] There have been only a few investigations considering an Auger decay of free excitons at shallow impurity centers.[20–22]

In the present paper we will present a quantitative calculation of the properties of the excitonic Auger capture mechanism. The paper is subdivided into the following sections. First we will elucidate the basic idea of our new model and give the equations necessary to calculate the transition probability. Then, a general calculation without any detailed assumptions about the impurity wave functions will be carried out. In order to get quantitative results, several approximations concerning the wave functions involved will then be introduced. The dependence of the capture coefficients on carrier density and temperature will be investigated in the next section. Finally, the results of the calculation will be compared to our experimental results reported earlier.[14]

II. BASIC CONCEPTS

The basic processes of an excitonic Auger recombination via a deep impurity level are sketched in Fig. 1. The capture of an electron into the deep level, for example, may occur when a free exciton meets the impurity. The electron from the exciton is captured by the impurity, whereas the excess energy is transferred to the hole which is highly excited into the valence band. Analogously, a hole may be captured into the deep level thereby exciting the electron into the conduction band. The complete recombination of an electron-hole pair requires, of course, the successive capture of an electron and a hole by the impurity, just as usually envisioned for Shockley-Read-Hall recombination.[2,3] We shall refer to such capture processes as "excitonic Auger capture" throughout this paper.

It is also possible that the electron and the hole of the exciton recombine transferring their energy to the parti-

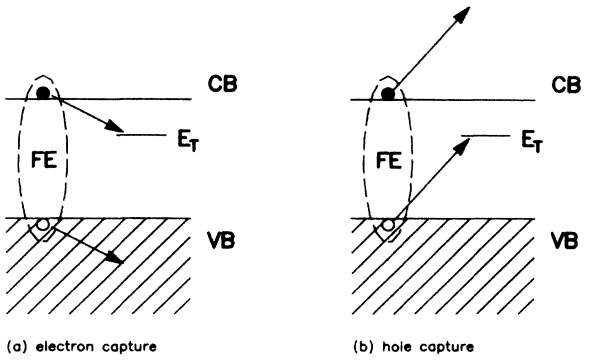

FIG. 1. Excitonic Auger capture processes into deep impurity level E_T. One particle out of the free exciton (FE) is captured, transferring its excess energy to the other one.

cle bound to the impurity (an electron or a hole). In effect, this is equivalent to the capture of a hole or an electron, respectively, by the impurity. However, we shall show below that the probability of these processes is much lower than that of the direct excitonic capture described in the preceding paragraph, so that they can be neglected.

Processes like the ones outlined above are known in scattering theory as "rearrangement collisions." For instance, the excitonic Auger capture of an electron by an impurity is quite similar to the scattering of a proton by a hydrogen atom where the electron is picked up by the incident proton. Collision processes of this kind differ from simple two-particle collisions in that the total Hamiltonian of the system has to be split up into a steady-state part and a perturbation in different ways for the initial and for the final state of the process. For a reaction $a+b\rightarrow c+d$ one may write[23]

$$H=H_{ab}+H'_{ab}=H_{cd}+H'_{cd} \ . \tag{1}$$

The transition probability from the initial to the final state can be written as[23]

$$W=\frac{2\pi}{\hbar}\int d^3k \ |M(\mathbf{k})|^2\delta(E_i-E_f)z(\mathbf{k}) \ . \tag{2}$$

Here, $M(\mathbf{k})$ is the transition matrix element, $z(\mathbf{k})$ is the density of states in $\mathbf{k}$ space of the final state, and the δ function between the initial energy E_i and the final energy E_f enforces energy conservation. Assuming parabolic energy bands and an isotropic matrix element one obtains

$$W=\frac{2m\kappa}{\pi\hbar^3}|M(\kappa)|^2 \ , \tag{3}$$

where κ is the wave vector in the final state.

The *exact* matrix element $M(\mathbf{k})$ is given by[23]

$$M(\mathbf{k})=\langle u_{cd}|H'_{cd}|\chi^+_{ab}\rangle=\langle\chi^-_{cd}|H'_{ab}|u_{ab}\rangle \ , \tag{4}$$

where u_{cd} and u_{ab} are the solutions of H_{cd} and H_{ab}, respectively, and χ^+_{ab} and χ^-_{cd} are the outgoing and incoming solutions of the full Hamiltonian. The two expressions for the matrix element (4) are usually referred to as the "post" and "prior" forms of the transition matrix element. In a first approximation (Born approximation), one may replace the exact wave functions χ^+_{ab} and χ^-_{cd} by the zero-order functions, getting[23]

$$M(\mathbf{k})\simeq\langle u_{cd}|H'_{cd}|u_{ab}\rangle\simeq\langle u_{cd}|H'_{ab}|u_{ab}\rangle \ . \tag{5}$$

Let us now demonstrate the calculation for the case of an electron being captured into a positively charged ionized donorlike impurity. Such an Auger process involves an exciton and a charged impurity core in the initial state and an electron bound to the impurity and a highly excited hole in the final state. The complete Hamiltonian that describes the electron, the hole, and the impurity contains a background term H_0 plus the three interaction terms shown schematically in Fig. 2(a), so that

$$\begin{aligned}H&=(H_0+U_{12})+(V_1+V_2)\\&=(H_0+V_1)+(U_{12}+V_2)\end{aligned} \tag{6}$$

in the spirit of Eq. (1).

We note that this Hamiltonian consists of contributions of the electron-electron interaction as well as of the electron-impurity interaction. In most previous investigations of Auger processes involving deep impurity states[7–13] only the electron-electron interaction has been considered as a perturbation causing the transition. There is, however, no *a priori* reason why the electron-impurity interaction should not be able to induce such a nonradiative transition. Therefore, we will treat the electron-electron and the electron-impurity interaction on an equal basis throughout this paper.

The transition matrix element in the Born approximation may now be written as

$$M\simeq\langle I^\kappa_k|V_2+U_{12}|x^K_i\rangle\simeq\langle I^\kappa_k|V_2+V_1|x^K_i\rangle \ , \tag{7}$$

where $|x^K_i\rangle$ is an eigenstate of H_0+U_{12} (an exciton) and $|I^\kappa_k\rangle$ is an eigenstate of H_0+V_1 (the electron bound to the impurity plus the highly energetic hole). We actually perfer the post form of the matrix element over the prior form since it does not involve an explicit expression for the electron-impurity interaction. We note that the use of all three interactions of Fig. 2(a) in the matrix element in previous work[20–22] appears to be incorrect in

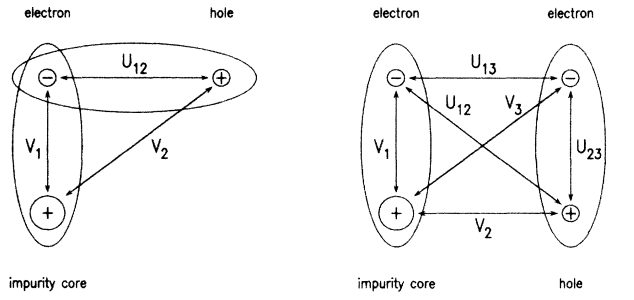

FIG. 2. Interactions between the particles participating in excitonic Auger capture processes.

the light of rearrangement scattering theory.[23]

The next step is to give explicit wave functions for $|x_i^K\rangle$ and $|I_k^\kappa\rangle$. The eigenstates of a free exciton with a center-of-mass momentum K are expanded in terms of eigenstates of the crystal by[24]

$$|x_i^K\rangle=\psi^i(r_1,r_2)u_{c,k_1}(r_1)u_{v,k_2}(r_2)$$
$$=\frac{1}{V_0^{1/2}}\sum_\beta A^i_{K,\beta}e^{i\beta r_1}e^{i(K-\beta)r_2}u_{c,\beta}(r_1)u_{v,K-\beta}(r_2)\ , \tag{8}$$

with $u_{c,k}(r_1)$ and $u_{v,k}(r_2)$ being the periodic parts of the Bloch functions. $A^i_{K,\beta}$ is the Fourier transform of the "internal" wave function $\psi^i_x(r_1,r_2)$ of the exciton.

The final state $|I_k^\kappa\rangle$ is described by a product of the wave functions of the electron bound to the impurity and that of a highly excited hole. In general, the wave function of the electron bound to the impurity is a superposition of all Bloch functions of the crystal[25]

$$\phi_t^j(r_1)=\frac{1}{V_0^{1/2}}\sum_{n,k}C^j_{n,k}e^{ikr_1}u_{n,k}(r_1)\ , \tag{9}$$

whereas the highly excited hole with momentum κ is described by

$$\phi_{2'}(r_2)=e^{i\kappa r_2}u_{v,\kappa}(r_2)\ . \tag{10}$$

Finally, the interaction potentials between the particles are of the form

$$V(r)=\frac{e^2}{\epsilon r}e^{-k_s r}\ . \tag{11}$$

In order to take into account many-particle effects in a simple approximation, we have used a screened Coulomb potential with a screening vector k_s for this interaction.

Now we have all the prerequisites to calculate the transition matrix element M. Using the wave functions and interaction potentials given above, we finally get (for details refer to subsection 1 of the Appendix, where the calculation of the first term is carried through in detail; the other term is completely analogous)

$$M=M_2+M_{12}$$
$$=\frac{4\pi e^2}{\epsilon V_0}\sum_\beta\frac{A^i_{K,\beta}F^1_{vv}C^{k*}_{c\beta}}{k_s^2+(K-\kappa-\beta)^2}-\frac{4\pi e^2}{\epsilon V_0}\sum_\beta\frac{A^i_{K,\beta}F^1_{vv}}{k_s^2+(K-\kappa-\beta)^2}\sum_n C^{k*}_{n,K-\kappa}F^2_{nc}$$
$$=\frac{4\pi e^2}{\epsilon V_0}\sum_\beta\frac{A^i_{K,\beta}F^1_{vv}}{k_s^2+(K-\kappa-\beta)^2}\left[C^{k*}_{c\beta}-\sum_n C^{k*}_{n,K-\kappa}F^2_{nc}\right]\ . \tag{12}$$

Here, F_{nm} denotes an overlap integral between the bands n and m, e.g.,

$$F^1_{vv}=\frac{1}{V_0}\int d^3r_2 u^*_{v,\kappa}u_{v,K-\kappa}\ . \tag{13}$$

From the above form of the matrix element, which does not contain any special assumptions about the shape of the wave functions, several general conclusions can be drawn. First, we note that, since *interband* overlap integrals are much smaller than *intraband* ones[27] (i.e., $F_{nc}\simeq\delta_{nc}$) even for the second term of the matrix element which contains a sum over the contributions of all bands, the conduction-band contribution to the impurity wave function ($C_{c,K-\kappa}$) will dominate. Thus we can conclude that electron capture into deep levels by an excitonic Auger process is by far dominated by the conduction-band portion of the impurity wave function.

For hole capture, on the other hand, the picture is somewhat different. For this case, the interactions between the particles involved are depicted in Fig. 2(b). The complete Hamiltonian for that system reads

$$H=(H_0+V_1+U_{23})+(V_2+V_3+U_{12}+U_{13})$$
$$=(H_0+V_1+V_3+U_{12}+U_{13}+U_{23})+(V_2)\ . \tag{14}$$

The initial state consists of an exciton and an electron bound to the impurity. In the final state only a hot electron is left. Even though the electron 1 and the hole 2 have already recombined in the final state, we still need to include their interactions with electron 3 and with the impurity in order to make the Hamiltonian consistent (of course, these interactions cancel out in the final state). Again, we choose the prior form of the transition matrix element which means that we have to calculate the matrix element of V_2 (the details of the calculation are completely analogous to the calculation shown in subsection 1 of the Appendix)

$$M=\langle f\mid V_2\mid i\rangle$$
$$=-\frac{4\pi e^2}{\epsilon V_0}\sum_\beta\frac{A_{K,\beta}F_{cc}C_{v,K-\beta}}{k_s^2+(\kappa-\beta)^2}\ . \tag{15}$$

In this case, only the valence-band contribution to the impurity wave function enters into the matrix element. Thus one may conclude that for an effective recombination center the wave functions must be constructed from comparable contributions from the valence band and from the conduction band. This is usually the case for deep impurities, whereas shallow donors or acceptors being described satisfactorily by effective-mass theory[26] are coupled to one band only and therefore do not contribute to the recombination.

Let us finally consider the processes mentioned briefly in the introduction to this section, namely capture pro-

cesses where the electron and the hole recombine transferring their energy to the particle bound at the impurity, which is either an electron or a hole. The calculations for these processes can be carried through in a straightforward manner, similarly as demonstrated here. However, all the matrix elements in these cases contain *interband* overlap integrals instead of the *intraband* ones in the matrix elements above (i.e., F_{cv} instead of F_{vv} or F_{cc}), since they always involve a direct transition of an electron from the conduction band to the valence band. Since interband overlap integrals are very small compared to intraband overlap integrals,[27] we will neglect this kind of processes in the further discussion.

III. APPROXIMATIONS AND RESULTS FOR THE EXCITONIC GROUND STATE

In order to get quantitative results, we have to introduce some approximations concerning the expansion coefficients C_{nk} of the impurity wave function and $A_{K,\beta}$ for the exciton wave function. In addition, the overlap integrals have to be estimated. For simplicity, we assume that the overlap integrals containing functions of the same band are equal to unity, whereas those with functions of different bands vanish[27]

$$F_{nm}=\delta_{nm} \ . \tag{16}$$

Furthermore, we need the Fourier coefficients of the exciton wave function. For isotropic parabolic bands the exciton wave function in real space may be written as (with R being the center-of-mass coordinate and ρ the coordinate of relative motion)

$$\psi^{1s}(R,\rho)=e^{iKR}\left[\frac{\alpha^3}{\pi}\right]^{1/2}e^{-\alpha\rho} \ . \tag{17}$$

Here, K is the center-of-mass momentum of the exciton, whereas the reciprocal Bohr radius α determines the extension of the exciton wave function (μ denotes the reduced mass of the exciton)

$$\alpha=\frac{\mu e^2}{\epsilon\hbar^2} \ . \tag{18}$$

Using this wave function we get the Fourier coefficients

$$A^{1s}_{K,\beta}=\left[\frac{\alpha^3}{\pi}\right]^{1/2}\frac{8\pi\alpha}{\left[\alpha^2+\left[\beta-\frac{m_e}{M}K\right]^2\right]^2} \ . \tag{19}$$

The most difficult problem remaining now is to get a realistic yet simple approximation for the wave function of the electron deeply bound to the impurity. Since an *a priori* calculation of the impurity wave function is beyond the scope of the present investigation, we use two simple models frequently employed in the literature. Some of the general results of a more realistic theory,[25,28–31] however, can be transferred to these simple models. The most important one appears to be the fact that for deep impurities there is no direct relation between the energetic position of the impurity level and the spatial localization of the impurity wave function.[32]

For further discussion we use the δ-potential model of Lucovsky[33] and a scaled effective-mass model.[8,9] In the δ-potential model, the localized impurity potential is approximated by a δ function. The respective wave function with the localization parameter γ reads as

$$\phi^{\delta}_t(r)=\left[\frac{\gamma}{2\pi}\right]^{1/2}\frac{1}{r}e^{-\gamma r} \ . \tag{20}$$

For comparison, an effective-mass wave function (1s hydrogen wave function) which is scaled to the appropriate localization[8,9] is also discussed

$$\phi^{1s}_t(r)=\left[\frac{\gamma^3}{\pi}\right]^{1/2}e^{-\gamma r} \ . \tag{21}$$

These impurity wave functions yield the following Fourier coefficients:

$$C^{\delta}(\beta)=\left[\frac{\gamma}{2\pi}\right]^{1/2}\frac{4\pi}{\gamma^2+\beta^2} \ , \tag{22}$$

$$C^{1s}(\beta)=\left[\frac{\gamma^3}{\pi}\right]^{1/2}\frac{8\pi\beta}{(\gamma^2+\beta^2)^2} \ . \tag{23}$$

Putting these expansion coefficients and those of the exciton into the expression (12) for the matrix element of the electron capture, we get (for details see subsection 2 of the Appendix)

$$M^{\delta}=\frac{8\pi e^2\sqrt{2\gamma}\alpha^{3/2}}{\epsilon V_0}\frac{1}{\kappa}\frac{1}{\alpha^2-\gamma^2}\left[\frac{2\alpha}{\alpha^2-\gamma^2}\left[\arctan\frac{\kappa}{\gamma+k_s}-\arctan\frac{\kappa}{\alpha+k_s}\right]-\frac{\alpha^2+\kappa^2}{\gamma^2+\kappa^2}\frac{\kappa}{(\alpha+k_s)^2+\kappa^2}\right] \ , \tag{24}$$

$$M^{1s}=\frac{32\pi e^2\gamma^{3/2}\alpha^{3/2}}{\epsilon V_0}\frac{1}{\kappa}\left[\frac{4\alpha\gamma}{(\alpha^2-\gamma^2)^3}\left[\arctan\frac{\kappa}{\alpha+k_s}-\arctan\frac{\kappa}{\gamma+k_s}\right]\right.$$
$$\left.+\frac{\kappa}{(\alpha^2-\gamma^2)^2}\left[\frac{\gamma}{(\alpha+k_s)^2+\kappa^2}+\frac{\alpha}{(\gamma+k_s)^2+\kappa^2}\right]-\frac{\kappa}{(\gamma^2+\kappa^2)^2}\frac{\gamma}{(\alpha+k_s)^2+\kappa^2}\right] \ . \tag{25}$$

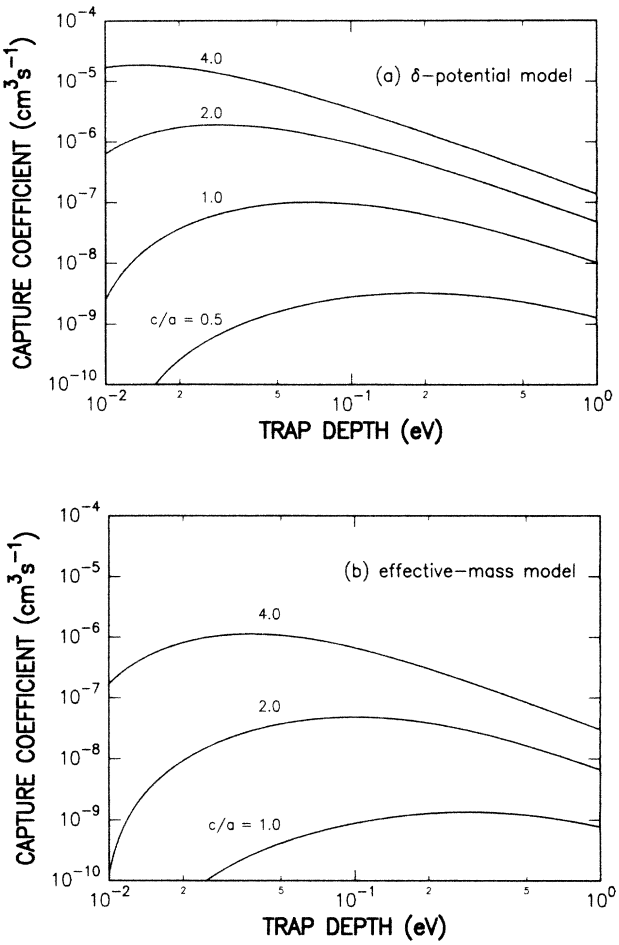

FIG. 3. Capture coefficient for an excitonic Auger process vs trap depth with the localization parameter c of the impurity wave function given in units of the lattice constant a. (a) δ-potential impurity, (b) effective-mass-like impurity.

From these matrix elements we can easily calculate the transition probability and the capture coefficients for the excitonic Auger electron capture. The results for the capture coefficient as a function of the energetic depth of the impurity level are depicted in Fig. 3. These results will be discussed in detail in Sec. V.

The results for the corresponding hole capture coefficients will not be given in detail here. However, their behavior as a function of the energy of the impurity level and the localization of its wave function is quite similar to that of the electron capture case, as it is expected from the similar structure of the leading term of (12) and (15). The relative magnitude of the electron or hole capture coefficients of a particular impurity depends on the contributions of the conduction and valence band, respectively, to the impurity wave function. In order to answer this question, one really needs to calculate the electronic structure of the impurity from first principles.

IV. INFLUENCE OF TEMPERATURE AND CARRIER DENSITY ON THE TRANSITION PROBABILITY

The calculation of the transition probability of an excitonic Auger capture process given above is valid for the $1s$ ground state of the free exciton. There is no explicit dependence of this transition probability on temperature or carrier density. At finite temperatures, however, excited states of the exciton, including scattering states, which have a larger extension of the wave function, have to be taken into consideration. In addition, at finite carrier densities, many-particle effects, e.g., screening of the Coulomb interaction, are expected. The screening of the interaction potentials leads to a weakening of the excitonic binding and therefore to a decrease of the transition probability.

For a quantitative calculation of the temperature and density dependence of the capture coefficients we have to average the contributions of all the excited states of the exciton to the transition probability. For this purpose we need the energies and the wave functions of these excited exciton states. Since we are considering a system at finite carrier density, the exciton is no longer bound by a Coulomb potential but rather by a screened Coulomb potential (Debye potential[34]). Therefore we have to calculate the eigenvalues and eigenfunctions of the Hamiltonian

$$\left[-\frac{\hbar^2}{2\mu}\Delta-\frac{e^2}{\epsilon r}e^{-k_s r}\right]\psi(r)=E\psi(r)\ . \tag{26}$$

In general, this equation cannot be solved analytically, and numerical methods have to be used. After separating the radial and azimuthal parts of the equation,[23] we transform the radial equation to an integral equation by means of a Fourier transformation. In this way, we get the integral operator $H(k)$ which is then discretized yielding the matrix $H_{kk'}$ (in excitonic units, details are discussed in subsection 3 of the Appendix)

$$H_{kk'}=k^2\delta_{kk'}-\frac{1}{\pi}\ln\frac{k_s^2+(k+k')^2}{k_s^2-(k-k')^2}$$

$$+l(l+1)\min(k,k')\ . \tag{27}$$

This matrix was diagonalized numerically yielding the eigenvalues and the eigenfunctions of H in $\mathbf{k}$ space which are needed to calculate the transition matrix elements of an excitonic Auger process (12). The screening vector k_s is given by[35]

$$k_s^2=\frac{8\pi e^2 n}{\epsilon kT}\frac{f_{-1/2}}{f_{1/2}}\ , \tag{28}$$

where n is the carrier density and $f_{-1/2}$ and $f_{1/2}$ are the Fermi integrals of order $-\frac{1}{2}$ and $\frac{1}{2}$, respectively. Using the Fourier coefficients of the pair wave functions calculated in this way, we are able to calculate the transition probability for each eigenstate of the exciton. The total transition probability is then given by the thermal average over all eigenstates[36]

$$W_{\text{tot}}=\frac{1}{Z}\left[\sum_{\substack{n\\n<0}}\sum_{l}\sum_{m}e^{-(E_{nl}/kT)}W_{nlm}+4\pi\Delta k\sum_{\substack{n\\n>0}}\sum_{l}\sum_{m}e^{-(E_{nl}/kT)}W_{nlm}\right], \tag{29}$$

with

$$Z=\sum_{\substack{n\\n<0}}\sum_{l}(2l+1)e^{-(En_{nl}/kT)}\int_{V_0}d^3\rho\,|\,\phi(\rho)\,|^2+4\pi\Delta k\sum_{\substack{n\\n>0}}\sum_{l}(2l+1)e^{-(E_{nl}/kT)}\int_{V_0}d^3\rho\,|\,\psi(\rho)\,|^2\,. \tag{30}$$

In this way, the capture coefficient of a deep impurity for an excitonic Auger process was calculated as a function of carrier density and temperature in a first approximation

V. DISCUSSION OF THEORETICAL RESULTS

In this section we will discuss the influence of various parameters on the capture coefficients of deep impurities for an excitonic Auger process. These parameters are the energetic position of the impurity level, the localization of the impurity wave function, and the binding energy and the Bohr radius of the exciton. In addition, we will discuss the differences between the excitonic Auger process and the "classical" impurity Auger process of free carriers.

The effects of differently localized impurity wave functions on the electron capture coefficient of an ionized deep donor in silicon are shown in Fig. 3. Using effective extensions of the wave function (defined as the radius of the sphere which comprises 70% of the charge) of 0.5, 1, 2, or 4 lattice constants we have calculated the capture coefficients for (a) the δ potential and (b) a $1s$ hydrogenlike wave function. From qualitative considerations one expects that a stronger localization causes a larger extension of the wave functions in k space, which in turn should lead to an increase in transition probability since it is considered to facilitate k conservation. In contrast, the quantitative calculation yields a decrease of the capture coefficients with increasing localization. The reason for this surprising result is that for the excitonic Auger process, the localization of the electron and the hole within the exciton also plays an important role. The transition matrix element (12) contains a product of the Fourier transforms $A_{K,\beta}$ and $C_{c\beta}$ of the exciton and impurity wave functions, whose shape is governed by the less localized one of the wave functions (the exciton). The impurity wave function, which is more localized and has less variation in k space, merely enters with its amplitude at $k=0$ decreasing with increasing localization.

For both impurity models considered here, the basic trend of the transition probability versus localization relation is the same. The transition probability decreases approximately with the third power of the localization parameter γ

$$W\sim\gamma^{-3}\,. \tag{31}$$

The absolute values of the capture coefficients vary between about 10^{-9} and 10^{-5} $\text{cm}^3\,\text{s}^{-1}$ for the variation of the localization given above. This corresponds to capture cross sections between 10^{-16} and 10^{-11} cm^2.

The influence of the energetic position of the trap level, or equivalently the energy of the hot Auger particle, is relatively small. For deep centers, the transition probability varies approximately like

$$W\sim\Delta E^{-3/2}\,, \tag{32}$$

but for shallow levels ($\Delta E<0.1$ eV) with a strongly localized wave function there may be even an increase of W with ΔE. For trap depths between 0.1 and 1 eV the capture coefficients vary by about a factor of 30 which is reasonable for silicon. The excess energy of the carrier to be captured, therefore, has a much lower influence on the transition probability than the localization of the wave function. This is due to the fact that the decrease of the matrix elements with increasing κ is partially compensated by the increasing density of states for the highly excited Auger particle at high energies.

In earlier attempts to investigate impurity Auger processes theoretically,[7–11] the localization of the impurity wave function was always treated as being closely related to the trap depth. This coupling originates from effective-mass theory of shallow impurities[8,9] and leads to a strong dependence of the transition probability on the trap depth. In contrast, deep impurities cannot be described properly be effective-mass theory, and contributions of many bands have to be taken into account.[25] The energetic position of the trap level is the result of a delicate cancellation of many contributions and is not directly related to the localization of the wave function.[32] Therefore, we have treated the trap depth and its localization as independent thus obtaining a weaker dependence of the capture coefficients on trap depth.

As mentioned earlier, the extension of the exciton wave function in k space is one key quantity for momentum conservation in the Auger process. The transition probability increases with the third power of α (a_0 is the Bohr radius of the exciton).

$$W\sim\alpha^3=\frac{1}{a_0^3}\,. \tag{33}$$

Therefore, large capture coefficients are expected in the case of silicon having a relatively small free exciton Bohr radius [$a_0=4.6$ nm (Ref. 37)].

The binding energy of the exciton does not enter directly into the expression for the transition probability of the exciton ground state. However, since the binding energy determines the thermal stability of the exciton, it strongly influences the temperature dependence of the capture coefficients. Roughly speaking, the slope of the decrease of the capture coefficients at a high temperature

is given by the exciton binding energy.

The temperature dependence of the capture coefficients calculated for a δ-potential trap by the procedure given in Sec. IV is depicted in Fig. 4. To simplify the understanding of the various effects involved in the temperature dependence, we have done the calculation for two different values of the carrier density with and without screening of the Coulomb interaction. At high temperature, the results behave just as expected qualitatively. Due to the increasing occupation level of highly excited states of the exciton, which are less localized, the capture coefficients decrease towards higher temperature.

Without screening of the Coulomb interaction, the capture coefficient remains constant at low temperature since all electron-hole pairs are bound forming free excitons. If screening is taken into account, the capture coefficient decreases towards zero temperature. This is due to the fact that (at a given carrier density) the screening vector k_s is inversely proportional to temperature, thus leading to a weakening of the excitonic binding at low temperature.

The dependence of the capture coefficients on the carrier density, which is shown in Fig. 5, includes two counteracting effects: On one hand, the statistical weight of the continuum states becomes larger at low carrier density. At high temperature, this should lead to a linear decrease of the capture coefficients with decreasing carrier density. On the other hand, the screening of the Coulomb interaction at high carrier density causes a decrease of the capture coefficients. In particular, this is the case at low temperature (e.g., 10 K) where the capture coefficients are up to 10 times smaller at intermediate densities (10^{16}–10^{17} cm^{-3}) than in the low-density limit. At still higher carrier densities, the capture coefficient increases again since the mean distance between free carriers then becomes smaller than the exciton Bohr radius.

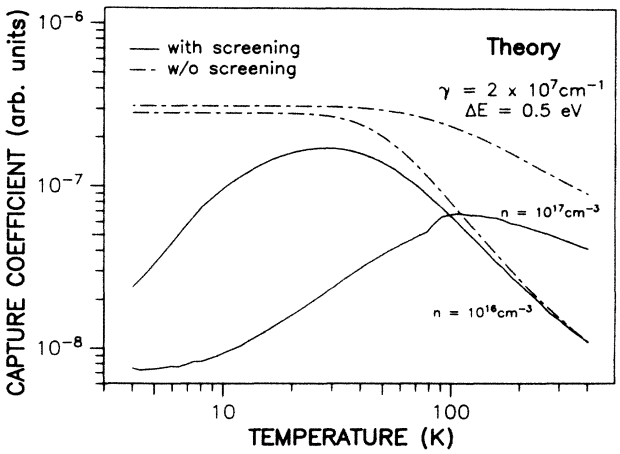

FIG. 4. Capture coefficients for the excitonic Auger process as a function of temperature for two different carrier densities. For clarity, the capture coefficients were calculated with and without screening of the Coulomb interaction of electrons and holes.

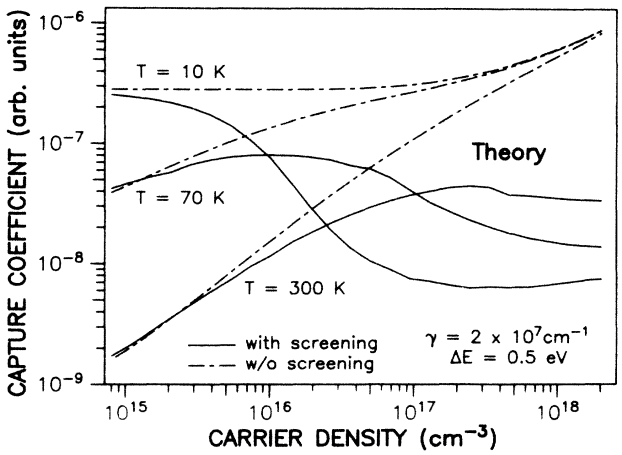

FIG. 5. Capture coefficients for the excitonic Auger process vs carrier density at three temperatures.

Compared to classical impurity Auger capture processes of free carriers,[7–11] the excitonic Auger process exhibits some remarkable differences. Whereas for the classical process no significant influence of temperature is expected,[7–11] the excitonic process is rather sensitive to temperature. The classical Auger process is always subject to a strong dependence on carrier density, contrary to the excitonic one, which gives a density independent capture coefficient at least at low temperature. At a given carrier density the transition probability for the excitonic process is usually much larger than that for the classical one due to the strongly enhanced local carrier density within the excitons.

VI. COMPARISON WITH EXPERIMENTAL RESULTS

The basic idea of excitonic Auger recombination via deep impurity levels in semiconductors treated theoretically in this paper was developed from our experimental results on recombination via deep levels in silicon.[14] We will now compare the results of our theory with the experimental data.

A. Capture coefficients

Let us start with a comparison of the absolute values of the capture coefficients. For the excitonic ground state (i.e., at low temperature and moderate carrier density), the theory yields a capture coefficient of the order 10^{-8}–10^{-5} $cm^3 s^{-1}$ within reasonable limits of the localization of the impurity wave function. On the other hand, the capture coefficients determined experimentally[14] are of the order 10^{-7}–10^{-6} $cm^3 s^{-1}$ at low temperature. This comparison shows that even the simple models used in our calculations lead to results within the correct order of magnitude.

Another interesting point is the ratio of electron capture to hole capture which can be derived qualitatively from theory in some special cases. Let us consider the case of gold in silicon here. As shown by Fazzio *et al.*[29] in a recent paper, the t_2 state of the substitutional gold in the forbidden gap is mostly *p*-like. Since the band

states near the top of the valence band are p-like too (in contrast to the s-like conduction band), we may assume that the impurity wave function is mostly composed of valence band states in this case. Using the general results for the transition matrix element given in Sec. II, we conclude that the capture of holes into this level should be more efficient than electron capture. This is in excellent agreement with the experimental results which indeed show that hole capture into the gold donor level is more efficient than electron capture.[14,38]

B. Temperature dependence

The temperature dependence of the carrier lifetime in silicon doped with deep recombination centers was one of the key experimental results for the development of our model. It was discussed in detail in Sec. IV A of Ref. 14. For a comparison with theory, the results obtained from high resistivity samples are suited best, since no modification of the real temperature dependence by bound exciton formation is expected.[14] Since the experimental lifetime values have always been evaluated in the low excitation limit, it is well justified to calculate the theoretical curve in this limit as well, i.e., to neglect the screening of the Coulomb interaction by free carriers at high carrier density.

In Fig. 6 the experimentally obtained temperature dependence of the carrier lifetime in the case of Si:Fe is compared to the results of our theory. The absolute value of the carrier lifetime at low temperature has been fitted to the experimental data since theory contains too many unknown parameters to give *a priori* values of the lifetime. However, as easily seen, we obtain excellent agreement between experiment and theory.

C. Majority carrier density

Experimentally, we have found that the capture coefficients of deep impurities for electrons and holes are independent of majority carrier density for temperatures between 70 and 300 K.[14] At least at low temperature the results of our theory are in good agreement with this finding: At 70 K there is in fact only a weak variation

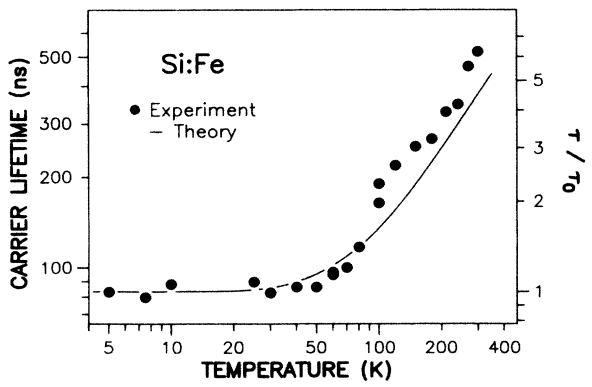

FIG. 6. Comparison between experimental temperature dependence of the carrier lifetime (Ref. 14) and that calculated for excitonic Auger recombination. The right-hand scale gives the lifetime normalized to its low-temperature limit.

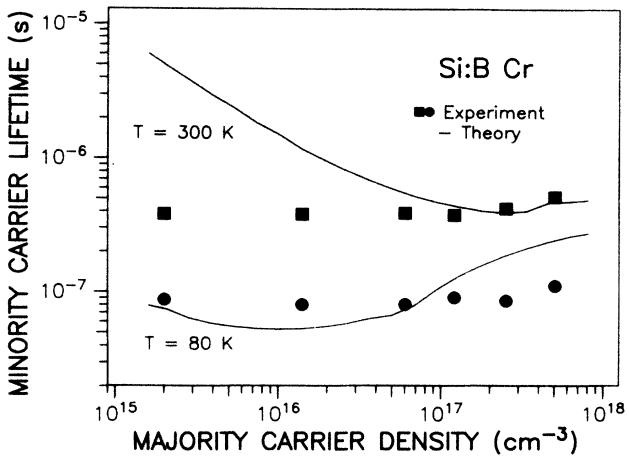

FIG. 7. Comparison between measured (Ref. 14) and calculated carrier density dependence of the carrier lifetime. (Sample prepared from silicon doped with boron as shallow dopant.)

of the capture coefficients with carrier density as calculated for an excitonic Auger process (Fig. 7). At higher temperatures (e.g., room temperature), however, the calculated carrier lifetime increases towards lower density below 10^{17} cm^{-3} which is clearly not observed experimentally. This increase is to be attributed to the exciton formation process which is a bimolecular reaction leading to a higher probability of exciton formation at larger carrier densities.

Whereas at low temperature the experimental results on the carrier density dependence of the recombination are reasonably described by our theory, there is some discrepancy at room temperature. This discrepancy may be attributed to the approximations involved in our theory. A better treatment of the many-particle effects occurring at high carrier density[39,40] within our theory should lead to a better agreement between theory and experiment.

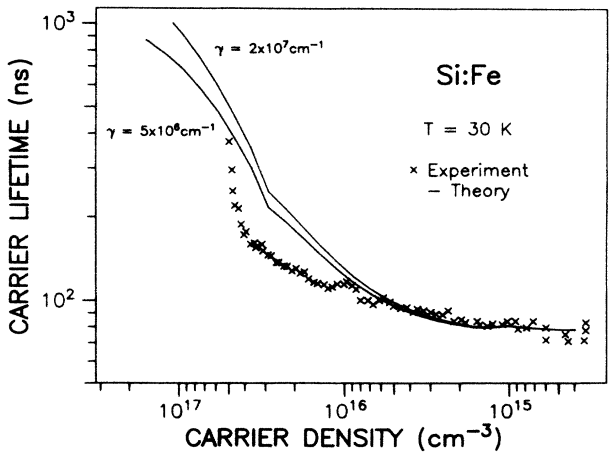

FIG. 8. Carrier lifetime vs carrier density near the Mott transition in a high excitation experiment (Ref. 14). The theoretical curves for excitonic Auger recombination are calculated for two values of the impurity localization γ.

D. Excitation dependence at low temperature

The behavior of the recombination via deep levels under strong optical excitation has been investigated at low temperature ($T<60$ K).[14] The main experimental result was that at high excitation the recombination becomes considerably slower than at low excitation.

The result of a typical measurement on iron-doped silicon at 30 K is shown in Fig. 8. For this figure, the original intensity versus time data[14] have been converted to a lifetime versus carrier density plot in order to simplify the comparison with theoretical results. The lifetime values were obtained by fitting an exponential to the neighborhood of every data point, whereas the absolute value of the initial carrier density was estimated from the experimental excitation conditions.

The solid lines in Fig. 8 were calculated from our theory for two values of the impurity localization parameter γ. We obtain a good qualitative agreement of the calculated curves with the experimental result. In theory as well as in the experiment there is a considerable increase of the lifetime for carrier densities above 10^{16} cm^{-3}.

It is interesting to compare these results with the so-called "Mott criterion"[41,42] which should give the upper density limit for the existence of free excitons. At 30 K, as realized in this case, the "Mott density" is about 5×10^{16} cm^{-3}. From Fig. 8 we readily see that even at densities below this limit an increase in carrier lifetime takes place. This is because even below the Mott density the binding energy and the localization of the excitons decrease smoothly. Above the Mott density the Coulomb enhancement of the Auger transition rate is further reduced accompanied by an increase in lifetime.

At lower temperature, in the region of electron-hole droplet (EHD) condensation, the experiments revealed[14] that the recombination of the EHD, which is normally determined by band-to-band Auger recombination,[43] shows no significant influence of the impurities whereas the free exciton lifetime is strongly shortened. This is also reproduced by our theory which predicts that the capture coefficients of the recombination centers are lower by more than a factor of 10 for the high-density EHD ($n=3.5\times10^{18}$ cm^{-3}) (Ref. 44) than for a low-density excitonic phase.

VII. CONCLUSION

In this paper we have presented a theoretical study of the properties of excitonic Auger capture processes into deep impurity levels in semiconductors. This investigation was strongly motivated by our experimental results indicating that such excitonic Auger processes are the dominating recombination mechanism in silicon containing deep recombination centers.[14] We have derived the general formulas for the matrix elements of excitonic Auger capture. Using two simple impurity models, namely Lucovsky's δ-potential model[33] and a scaled effective-mass model,[8,9] we have quantitative estimates for the capture coefficients. In order to study the influence of temperature and carrier density on excitonic Auger processes we have also included some many-body effects (screening of the Coulomb interaction) in a simple approximation.

Generally the results of our calculations are in excellent agreement with our experimental results reported earlier.[14] This confirms our argument that excitonic Auger capture is one of the most important mechanisms for nonradiative recombination via deep impurity levels in semiconductors.

ACKNOWLEDGMENTS

The author is indebted to W. Schmid, A. Haug, G. Mahler, and M. Pilkuhn for stimulating discussions. This work was in part supported by the Bundesministerium für Forschung und Technologie (BMFT) under Contract No. NT-2617.

APPENDIX

1. General results

The derivation of the matrix elements for excitonic Auger capture into deep impurity levels is now demonstrated for the case of the capture of an electron into a donorlike center. The analogous cases of hole capture and of acceptorlike centers may be treated in a similar way.

By inserting the wave functions (8), (9), and (10) as well as the interaction potential V_2 (11) into the general expression (7) for the matrix element we get for the leading term

$$M_2=\frac{1}{V_0}\int d^3r_1 d^3r_2\left[\sum_{n,\beta'} C^*_{n\beta'} e^{-i\beta' r_1} u^*_{n\beta'}(r_1)\right] e^{-i\kappa r_2} u^*_{v\kappa}(r_2)\frac{e^2 e^{-k_s r_2}}{\epsilon r_2}\left[\sum_{\beta} A_{K,\beta} e^{i\beta r_1} u_{c\beta}(r_1) e^{i(K-\beta)r_2} u_{v,K-\beta}(r_2)\right]. \tag{A1}$$

Now we exchange the integrations over r and β, getting

$$M_2=\frac{1}{V_0}\sum_{n,\beta'}\sum_{\beta} C^*_{n\beta'} A_{K,\beta}\int d^3r_1 d^3r_2 e^{-i\beta' r_1} u^*_{n\beta'}(r_1) e^{-i\kappa r_2} u^*_{v\kappa}(r_2)\frac{e^2 e^{-k_s r_2}}{\epsilon r_2} e^{-\beta r_1} u_{c\beta}(r_1) e^{i(K-\beta)r_2} u_{v,K-\beta}(r_2). \tag{A2}$$

The integral over r_1 can be executed immediately, yielding

$$M_2=\frac{1}{V_0}\sum_{n,\beta'}\sum_{\beta} C^*_{n\beta'} A_{K,\beta}\delta_{nc}\delta_{\beta\beta'}\int d^3r_2 e^{-i\kappa r_2} u^*_{v\kappa}(r_2)\frac{e^2 e^{-k_s r_2}}{\epsilon r_2} e^{i(K-\beta)r_2} u_{v,K-\beta}(r_2). \tag{A3}$$

In order to calculate the remaining integral over r_2, the Bloch factors u_{vk} are expressed by a Fourier series

$$u_{vk}(r)=\sum_L B_{vL}(k)e^{iLr} , \tag{A4}$$

now allowing for the calculation of the integral I over r_2

$$I=\sum_{L,L'} B^*_{vL}(\kappa)B_{vL'}(K-\beta)\frac{4\pi e^2}{\epsilon} \times\frac{1}{k_s^2+(K-\beta-\kappa-L-L')^2} . \tag{A5}$$

Applying a usual approximation,[7] we assume that the main contribution to this integral comes from the first Brillouin zone, i.e., $L=L'=0$, getting

$$M_2=\frac{4\pi e^2}{\epsilon}\sum_\beta \frac{A_{K,\beta}F^1_{vv}C^*_{c\beta}}{k_s^2+(K-\kappa-\beta)^2} , \tag{A6}$$

with the overlap integral

$$F^1_{vv}=\frac{1}{V_0}\int d^3r\, u^*_{v\kappa}(r)u_{v,K-\beta}(r) . \tag{A7}$$

2. Special impurity models

The calculation of the transition matrix element for an exciton in the 1s ground state and a δ-potential impurity proceeds from expression (12). Since the overlap integral F_{vv} contains only functions of the same band it is set to unity.[27] The Fourier coefficients of the 1s exciton wave function reads as

$$A_{K,\beta}=\left[\frac{\alpha^3}{\pi}\right]^{1/2}\frac{8\pi\alpha}{[\alpha^2+(K-\beta)^2]^2} , \tag{A8}$$

whereas those of the impurity wave function (δ-potential model) are given by

$$C^*_{c\beta}=\left[\frac{\gamma}{2\pi}\right]^{1/2}\frac{4\pi}{\gamma^2+\beta^2} . \tag{A9}$$

If we neglect the center-of-mass motion of the exciton ($K=0$) we get for the matrix element

$$M=\frac{16e^2}{\epsilon V_0}\left[\frac{\alpha^3}{\pi}\right]^{1/2}\left[\frac{\gamma}{2\pi}\right]^{1/2}\int d^3\beta\frac{1}{k_s^2+(\kappa+\beta)^2}\frac{1}{(\alpha^2+\beta^2)^2}\frac{1}{\gamma^2+\beta^2}\frac{\kappa^2-\beta^2}{\gamma^2+\kappa^2} . \tag{A10}$$

After performing the angular integration this yields

$$M=\frac{16\pi e^2}{\epsilon\kappa V_0}\left[\frac{\alpha^3}{\pi}\right]^{1/2}\left[\frac{\gamma}{2\pi}\right]^{1/2}\int_0^\infty d\beta\frac{\beta}{(\alpha^2+\beta^2)^2}\frac{1}{\gamma^2+\beta^2}\ln\frac{k_s^2+(\kappa+\beta)^2}{k_s^2+(\kappa-\beta)^2}\frac{\kappa^2-\beta^2}{\gamma^2+\kappa^2} . \tag{A11}$$

The remaining integral over β requires a lengthy calculation, finally yielding

$$M=\frac{8\pi e^2\sqrt{2\gamma}\alpha^{3/2}}{\epsilon V_0}\frac{1}{\kappa}\frac{1}{\alpha^2-\gamma^2}\left[\frac{2\alpha}{\alpha^2-\gamma^2}\left[\arctan\frac{\kappa}{\gamma+k_s}-\arctan\frac{\kappa}{\alpha+k_s}\right]-\frac{\kappa}{(\alpha+k_s)^2+\kappa^2}\frac{\alpha^2+\kappa^2}{\gamma^2+\kappa^2}\right] . \tag{A12}$$

3. Effects of carrier density and temperature

In order to include the influence of carrier density and temperature into our calculation we need to know the exciton binding energy and wave function at finite carrier density. In a first approximation these are calculated by solving the Schrödinger equation for a particle in a screened Coulomb potential (in excitonic units)

$$\left[-\Delta-\frac{2}{r}e^{-k_s r}\right]\psi(\mathbf{r})=E\psi(\mathbf{r}) . \tag{A13}$$

This equation may be separated into radial and azimuthal parts. For the radial part we set

$$R(r)=\frac{1}{r}u(r) , \tag{A14}$$

yielding

$$\left[-\frac{d^2}{dr^2}-2\frac{e^{-k_s r}}{r}+\frac{l(l+1)}{r^2}\right]u(r)=Eu(r) . \tag{A15}$$

By means of a Fourier transformation this equation is converted into an integral equation which is discretized and solved numerically. Therefore we have to calculate the eigenvalues and eigenvectors of the matrix

$$H_{kk'}=k^2\delta_{kk'}-\frac{1}{\pi}\ln\frac{k_s^2+(k+k')^2}{k_s^2+(k-k')}+l(l+1)\min(k,k') . \tag{A16}$$

The computed eigenvalues give the energies of the exciton states and the corresponding eigenvectors may be inserted directly into the transition matrix element yielding the transition probability as a function of the quantum numbers.

[1]N. F. Mott, Solid State Electron. **21**, 1275 (1978).
[2]W. Shockley and W. T. Read, Phys. Rev. **87**, 835 (1952).
[3]R. N. Hall, Phys. Rev. **87**, 387 (1952).
[4]H. J. Queisser, Solid State Electron. **21**, 1495 (1978).
[5]T. N. Morgan, Phys. Rev. B **28**, 7141 (1983).
[6]V. N. Abakumov, V. I. Perel', and I. N. Yassievich, Fiz. Tekh. Poluprovodn. **12**, 3 (1978) [Sov. Phys.—Semicond. **12**, 1 (1978)].

[7]P. T. Landsberg, C. Rhys-Roberts, and P. Lal, Proc. Phys. Soc. London **84**, 915 (1964).
[8]D. J. Robbins and P. T. Landsberg, J. Phys. C **13**, 2425 (1980).
[9]A. Haug, Phys. Status Solidi B **97**, 481 (1980).
[10]A. Haug, Phys. Status Solidi B **108**, 443 (1981).
[11]D. J. Robbins, J. Phys. C **16**, 3825 (1983).
[12]G. F. Neumark, Phys. Rev. B **7**, 3802 (1973).
[13]F. A. Riddoch and M. Jaros, J. Phys. C **13**, 6181 (1980).
[14]A. Hangleiter, Phys. Rev. B **35**, 9149 (1987).
[15]M. Lax, Phys. Rev. **119**, 1502 (1960).
[16]A. Hangleiter, Phys. Rev. Lett. **55**, 2976 (1985).
[17]D. F. Nelson, J. D. Cuthbert, P. J. Dean, and D. G. Thomas, Phys. Rev. Lett. **17**, 1262 (1966).
[18]W. Schmid, Phys. Status Solidi B **84**, 529 (1977).
[19]S. A. Lyon, G. C. Osbourn, D. L. Smith, and T. C. McGill, Solid State Commun. **23**, 425 (1977).
[20]M. Trlifaj, Czech. J. Phys. B **14**, 227 (1964).
[21]M. Trlifaj, Czech. J. Phys. B **15**, 780 (1965).
[22]J. Singh and P. T. Landsberg, J. Phys. C **9**, 3627 (1976).
[23]L. I. Schiff, *Quantum Mechanics* (McGraw-Hill, New York, 1968).
[24]R. S. Knox, *Theory of Excitons* (Academic, New York, 1963).
[25]M. Jaros, *Deep Levels in Semiconductors* (Hilger, Bristol, 1982).
[26]W. Kohn, in *Solid State Physics,* edited by F. Seitz and D. Turnball (Academic, New York, 1957), Vol. 5, p. 257.
[27]E. Antoncik and P. T. Landsberg, Proc. Phys. Soc. London **82**, 337 (1963).
[28]M. Scheffler, in *Festkörperprobleme XXII,* edited by P. Grosse (Vieweg, Braunschweig, 1982), p. 115.
[29]A. Fazzio, M. J. Caldas, and A. Zunger, Phys. Rev. B **32**, 934 (1985).
[30]H. Katayama-Yoshida and A. Zunger, Phys. Rev. B **31**, 7877 (1985).
[31]F. Beeler, O. K. Andersen, and M. Scheffler, Phys. Rev. Lett. **55**, 1498 (1985).
[32]M. Jaros, Phys. Rev. B **16**, 3694 (1977).
[33]G. Lucovsky, Solid State Commun. **3**, 299 (1965).
[34]G. M. Harris, Phys. Rev. **125**, 1131 (1962).
[35]J. M. Ziman, *Principles of the Theory of Solids* (Cambridge University Press, Cambridge, 1969).
[36]G. Levich, *Theoretical Physics* (North-Holland, Amsterdam, 1971).
[37]The Bohr radius of free excitons is calculated from the experimental value of the exciton binding energy: $a_0=(\hbar^2/2\mu E_x)^{1/2}$ using $E_x=14.7$ meV as given by K. L. Shakley and R. E. Nahory, Phys. Rev. Lett. **24**, 942 (1970).
[38]R. H. Wu and A. R. Peaker, Solid State Electron. **25**, 643 (1982).
[39]P. Vashishta, P. Battacharyya, and K. S. Singwi, Phys. Rev. B **10**, 5108 (1974).
[40]H. Schweizer, A. Forchel, A. Hangleiter, S. Schmitt-Rink, J. P. Löwenau, and H. Haug, Phys. Rev. Lett. **51**, 698 (1983).
[41]N. F. Mott, *Metal Insulator Transitions* (Barnes and Noble, New York, 1974).
[42]N. F. Mott, Philos. Mag. B **37**, 377 (1978).
[43]W. Schmid, Phys. Status Solidi B **94**, 413 (1978).
[44]A. Forchel, B. Laurich, J. Wagner, W. Schmid, and T. L. Reinecke, Phys. Rev. B **25**, 2730 (1982).